Title page

Stereoselective Interaction of Pantoprazole with ABCG2:

I. Drug accumulation in rat milk

Lipeng Wang and Patrick J. McNamara

Department of Pharmaceutical Sciences, College of Pharmacy,

University of Kentucky, Lexington, KY, 40536

DMD Fast Forward. Published on February 16, 2012 as DOI: 10.1124/dmd.111.041608
This article has not been copyedited and formatted. The final version may differ from this version.

Running title page

a) Pantoprazole stereoselective interaction with Abcg2: *in vivo*

b) Corresponding Author: Dr. Patrick J. McNamara, Department of Pharmaceutical Sciences, College of Pharmacy, University of Kentucky, 789 South Limestone, 40536, USA; PH(859-257-8656); Email: pmcnamar@email.uky.edu

c) Text Pages: 25

Tables: 1

Figures: 4

References: 30

Supplementary figure: 0

Words in abstract: 246

Words in introduction: 745

Words in discussion: 1003

d) Abbreviations:

ABCG2/Abcg2: ATP binding cassette transporter family G member 2;

PAN: pantoprazole

GF120918: N-(4-[2-(1,2,3,4-tetrahydro-6,7-dimethoxy-2-isoquinolinyl)ethyl]-phenyl)-9,10-dihydro-5-methoxy-9-oxo-4-acridine carboxamide

Abstract

Active transport of drug into milk is a major concern in breastfeeding. Abcg2 plays a critical role in drug transfer into rat milk which is consistent with evidence in humans. Although it is estimated that about half of all therapeutic agents are chiral, there have been few reports of stereoselective interactions with ABCG2. The purpose of this study was to investigate the interaction of pantoprazole (PAN) isomers with Abcg2 in *in vitro* and *in vivo* experiments. Pantoprazole isomer flux was characterized using Abcg2 -MDCKII cells in Transwells. In a crossover design, lactating Sprague-Dawley lactating rats were used to study PAN accumulation in milk after an i.v. infusion of pantoprazole mixture after Abcg2 inhibitor (GF120918). Samples were analyzed by HPLC/LC-MS. The results indicated that pantoprazole isomers were transported in an identical fashion in vector-MDCKII cell lines, whereas a significant difference in flux was observed in Abcg2-MDCKII cell line. The administration of GF120918 slightly increased the concentration of both isomers in serum, but no statistical difference was observed. However, the systemic clearance of (+) PAN (0.57±0.1) was larger than (-) PAN (0.44±0.12) ($p<0.01$). Milk to serum ratio of (-) PAN (1.36±0.20) was 2.5 fold greater than that of (+) PAN (0.54±0.09) ($p<0.01$). Administration of GF120918 decreased M/S of (-) PAN to 0.50±0.08 ($p<0.001$) and (+) PAN to 0.38 ±0.07 ($p>0.05$). In conclusion, Abcg2 interacts stereoselectively with PAN isomers which is responsible for their differential accumulation in milk. Stereoselective transport of ABCG2 may have broader consequences in drug disposition.

Introduction

ABCG2 (ATP binding cassette transporter isoform G2) exhibits a broad substrate specificity transporting hydrophobic, anionic, and cationic drugs (Mao and Unadkat, 2005) and widely distributes in such tissues as kidney, liver, blood-brain barrier, placenta, stem cells and mammary gland and is reported to be of relevance in the absorption, distribution, elimination and toxicity of drugs (Oostendorp et al., 2009). ABCG2 plays a significant role in the accumulation of xenobiotics in milk (Jonker et al., 2005; Merino et al., 2006). Some dietary carcinogens, toxins and antibiotics that are substrates of ABCG2 are readily transported into milk and result in high M/S ratios (Merino et al., 2006; van Herwaarden et al., 2006). While other transporters may be present in lactating mammary epithelial cells (Alcorn et al., 2002), ABCG2 appears to be playing a prominent role in drug accumulation in milk. One hypothesis would hold that all viable ABCG2 substrates would exhibit high M/S ratio (greater than diffusion alone).

Pantoprazole (PAN) is a proton pump (H+/K+-ATPase) inhibitor (PPI) that binds specifically and irreversibly to the proton pump to reduce gastric acid secretion (McDonagh et al., 2009). PAN has been used as an inhibitor and a substrate of murine Bcrp1 (Breedveld et al., 2004). A case report described a M/S value of 0.022 for racemic PAN. While the clinical relevance of this finding is not definitive, PAN use in lactating women was regarded as safe given the low infant dose exposure (Plante et al., 2004). From a mechanistic perspective, the observation of such a low M/S ratio for an ABCG2 substrate is unclear and would appear to contradict the hypothesis that all such substrates would accumulate in milk. Perhaps PAN is not as good a substrate for human ABCG2 as was first thought and hence, diffusion and PAN extensive serum protein binding dominate the milk to serum ratio. Another confounding factor is that PAN is marketed as a racemate and the authors of the case report used did not measure

DMD Fast Forward. Published on February 16, 2012 as DOI: 10.1124/dmd.111.041608
This article has not been copyedited and formatted. The final version may differ from this version.

individual isomers. PAN has been shown to undergo enantioselective hepatic metabolism in both humans and rats (Tanaka et al., 2001; Xie et al., 2005). Poor metabolizers of S-mephenytoin (a CYP2C19 substrate) were less able to metabolize (+) PAN than (–) PAN (Tanaka et al., 2001). A marked difference in the intereraction of PAN isomers with ABCG2 could be playing a role in its limited M/S ratio.

It is estimated that about half of marketed therapeutic agents are chiral with most available as 50/50 mixtures of their enantiomeric forms (Andersson and Weidolf, 2008). The stereoselective metabolism as well as genetic polymorphisms of CYP450 and receptors can influence pharmacokinetics, pharmacodynamics, and toxicity (Katsuki et al., 2001; Tateishi et al., 2008; Miura and Uno). These differentiated interactions may be especially critical for those drugs that have a narrow therapeutic index (e.g., warfarin). Remarkably, there are limited reports of stereoselective interaction of drugs with transporters. Cetirizine exhibited moderate enantioselectivity in the absorptive and secretory flux across CaCo-2 monolayers, which was attributed to the interaction of the enantiomers with P-gp and MRP2 (He et al., 2009). Several *in vitro* and *in vivo* studies suggest an enantioselective drug transport at the human blood-brain barrier and implicate P-gp (Choong et al., 2010). However, it should be noted that this is not universal observation. No evidence was observed for stereoselective P-gp mediated transport of S- and R-enantiomers of venlafaxine and its major metabolites into murine brain (Karlsson et al., 2010). There are no reports of individual PAN isomers interacting with ABCG2 or any other transporter. There is but a single report of stereoselective drug accumulation in milk. The M/S ratio for the R enantiomers of fluoxetine (and its major metabolite, norfluoxetine) were 50% (40%) higher than the S enantiomers in lactating women (Kim et al., 2006). The authors

speculated this stereoselective distribution into milk was attributed to differences in the extent of protein binding of the enantiomers in milk compared with plasma (Kim et al., 2006).

Previously we have utilized Abcg2 expressed in a MDCKII cell line and a chemical knock-out Abcg2 rat model (Abcg2 inhibited by GF120918) to examine the role of Abcg2 in drug accumulation in milk (Wang et al., 2008). The purpose of the current paper was to establish whether any stereoselective differences of PAN isomers with rAbcg2 are manifested in the accumulation of PAN isomers in rat milk. The observations made in the current paper prompted further detailed *in vitro* characterization of PAN flux in another companion paper (Wang et al., 2011).

DMD Fast Forward. Published on February 16, 2012 as DOI: 10.1124/dmd.111.041608
This article has not been copyedited and formatted. The final version may differ from this version.

Materials and methods:

Chemicals. Protonix I.V (Pantoprazole sodium, 50:50 stereo mixtures) was obtained from Altana (Konstanz, Germany) and zonisamide sodium was purchased from Sigma-Aldrich (St. Louis, MO). The isomers of PAN were obtained from Altana Pharma AG (Konstanz, Germany). GF120918 was a gift from GlaxoSmithKline (Research Triangle Park, NC). All the organic solvents [high-performance liquid chromatography (HPLC) grade] were purchased from Thermo Fisher Scientific (Waltham, MA).

Animals. Five adult female lactating Sprague-Dawley rats (250–350 g) with 1- or 3-day-old pups were purchased from Harlan Laboratories (Indianapolis, IN). Animals were maintained under a 12/12-h light/dark cycle and had access to food and water during the experiments. The rats were acclimatized for at least 1 week before the experiment. All the procedures were approved by the University of Kentucky Institutional Animal Care and Use Committee.

Flux study. Rat Abcg2 and empty vector (pcDNA3.1) expressed in Madin-Darby Canine Kidney II Cells has been established in our lab (Wang et al., 2008). Cells were seeded on microporous membrane filters (3.0-μm pore size, 24-mm diameter; Transwell 3414; Corning Inc., Corning, NY) at a density of 1.0 x 10^6 cells/well. Cells were grown for 4 days to achieve transepithelial electrical resistance >200 Ω· cm2, and media was replaced every other day. Before the experiment, the media at both the apical and basolateral side of the monolayer was replaced with 2 ml of OptiMEM media (Invitrogen, CA) without serum. The apical or basolateral side was loaded with 25 μM if either (+) or (-) PAN isomer containing 0.2 μCi/ml [^{3}H]mannitol (Perkin Elmer, Norton, OH). Cells were incubated at 37°C in 5% CO_2. To assess tight junctions of each monolayer, 50 μl aliquots were collected to assess the paracellular flux of

DMD Fast Forward. Published on February 16, 2012 as DOI: 10.1124/dmd.111.041608
This article has not been copyedited and formatted. The final version may differ from this version.

[^{3}H] mannitol into the opposite compartment. For PAN isomers transport, 140-µl aliquots were taken at 1, 2, 3 and 4 h. Samples were stored at -80°C until the time of analysis.

***In vitro* M/S.** The contribution of passive diffusion on the M/S of PAN was estimated *in vitro* using Equation 1 (Fleishaker et al., 1987; Fleishaker and McNamara, 1988):

$$\left(\frac{M}{S}\right)_{predicted} = \left(\frac{f_S^u}{f_M^u}\right)\left(\frac{f_S}{f_M}\right)\left(\frac{W}{S}\right) \qquad \text{Eq. 1}$$

where f^u is the unionized fraction of drug in serum or milk, f is the free fraction of drug in serum or milk, W/S is the ratio of the drug concentration in whole milk to the drug concentration in skim milk, and the subscripts s and m represent serum and milk, respectively.

The W/S ratios, a measure of the partitioning of PAN isomers into milk fat, were determined following LC-MS analysis of PAN isomer concentrations in whole milk and skim milk into which isomer had been added. The unionized fraction in serum and skim milk, a measure of the pH partitioning of drug between serum and milk, was calculated from the pKa of each isomer and from the pH of serum (pH 7.45) and milk (pH 6.8)(Alcorn and McNamara, 2002). The unbound fraction of PAN isomers in milk and serum were determined by equilibrium dialysis of these fluids against a 0.133 M phosphate buffer (milk pH 6.8 and serum pH 7.45) in plexiglass dialysis cells (single place, 0.5 ml cells). After 8 hours equilibrium at 37^{o}C, samples were taken from both donor and recipient sides. These concentrations were determined by LC-MS.

***In vivo* studies.** The jugular and femoral veins of Sprague-Dawley lactating female rats were cannulated under ketamine/xylazine anesthesia on days 10 to 12 postpartum. A randomized cross over study design was used. Animals were randomized to receive an i.v. bolus pretreatment of GF120918 (10 mg/kg in DMSO) or with equivalent volume of DMSO

DMD Fast Forward. Published on February 16, 2012 as DOI: 10.1124/dmd.111.041608
This article has not been copyedited and formatted. The final version may differ from this version.

(approximately 0.15 ml) administered i.v. 10 minutes before an i.v. infusion of PAN in saline (0.4 mg/ml/h) for 8 h. All animals were crossed over on the second day to complete both phases of pretreatment (Wang et al., 2008). One milliliter of normal saline was given hourly by i.v. infusion to prevent dehydration during infusion. The dams were separated from the pups 4 hours before the infusion. Blood samples were drawn every 2 hours during the infusion. The blood samples were protected from light in separator tubes (BD Microtainer, Franklin Lakes, NJ), centrifuged to harvest serum, and frozen at -80°C until analysis. Milk samples were obtained by manual manipulation under light anesthesia (ketamine) at the end of the infusion. Milk samples were protected from light exposure, and frozen at -80°C until analysis.

Sample preparation for LC-MS. To each aliquot (50 µl) of serum, 10 µl 0.2 M NaOH and 20 µl of 10 µg/ml zonisamide sodium (internal standard) were added and the proteins were precipitated with 1ml Ethyl acetate, vortexed for 1 min, and then centrifuged at 2,400 rpm for 15 min at room temperature. The clear layer was collected into another clean glass tube (~0.8 ml) and dried under nitrogen in a 40^{o}C water bath. Samples were reconstituted in 50 µl mobile phase (15% Acetonitrille and 85% water but without formic acid). Each aliquot of 25 µl of milk was mixed with an equal volume of NaOH and zonisamide sodium. Protein was precipitated with 1 ml of cold methanol, vortexed for 30 seconds, and then centrifuged at 14,000g for 10 min at 4°C. The clear layer was collected to a clean glass tube (~0.9ml) and dried under nitrogen in a 40°C water bath. Samples were reconstituted in 200 µl water and mixed with 1 ml ethyl acetate was added. The extraction procedure was the same as serum samples. The collected clear layers were dried under nitrogen in a 40^{o}C water bath and reconstituted in 50 µl mobile phase. This method was adapted from Bharathi (Bharathi et al., 2009). PAN isomers in phosphate buffer samples from *in vitro* predicted M/S ratio experiment were reconstituted in 1 ml water and 2 ml ethyl

DMD Fast Forward. Published on February 16, 2012 as DOI: 10.1124/dmd.111.041608
This article has not been copyedited and formatted. The final version may differ from this version.

acetate, vortexed and centrifuged at 2400rpm for 15 min. The 1.8 ml organic layer was collected and dried under nitrogen at 40^{o}C water bath and reconstituted in 50 µl mobile phase.

Pantoprazole HPLC analysis (*in vitro* studies). Concentrations of total PAN were assayed by HPLC on a Luna RP18 125 x 4.0-mm column (Phenomenex, Torrance, CA). The analyte was eluted with 40% acetonitrile/60% 10 mM potassium phosphate buffer, pH 7.2, at 0.5 ml/min. PAN was detected by UV absorption (290 nm). Aliquots of PAN in Opti-MEM medium were directly injected onto the HPLC. The standard curve range was 7.8 to 2000 ng/ml. All the standard curves showed an intraday and interday variability of <10% and $r^2 > 0.999$.

Pantoprazole isomer analyses by LC-MS (in vivo). A Varian 1200L Triple Quadrupole mass spectrometer (Walnut Creek, CA) equipped with an electrospray ionization (ESI) source and a Varian MS Workstation (6.42) data system was employed. The interface was adjusted to the following conditions: positive ion mode; spray needle voltage, 5000V; shield voltage, 600V; capillary voltage, 40V; drying gas (Nitrogen) temperature, 300^{o}C. MS/MS spectra were obtained for selected precursor ions through incidental collision with neutral gas molecules (Argon) at 2.0mTorr in the collision cell of the mass spectrometer. The collision energy was set at 8.50V. The parameters of the selected reaction monitoring transitions for the [M+H]+ to selected product ions were optimized with the following typical values for the analytes and internal standard: PAN m/z 384 to 200 and the internal standard zonisamide m/z 213 to 132. The LC conditions were as follows. The column was a Lux 5 µl Amylose-2 150 x 4.60-mm Chiral column (Phenomenex, Torrance, CA). The initial mobile phase consisting of acetonitrile: water: formic acid (15%:85%:0.02%) was delivered by dual Varian ProStar 210 pumps (Walnut Creek, CA), at a flow rate of 0.3 ml/min. A gradient program was utilized; the acetonitrile phase was increased to 90% over 12 min and held constant for an additional 6 min. The acetonitrile phase

DMD Fast Forward. Published on February 16, 2012 as DOI: 10.1124/dmd.111.041608
This article has not been copyedited and formatted. The final version may differ from this version.

was returned to 15% over 1 min and held constant for an additional 11 min for a total run time of 30 min. The retention times of (+) PAN, (-) PAN and zonisamide were approximately 12.04, 13.05 and 12.01 minutes (Figure 2). The standard curve was linear from 80 to 5,000 ng/ml in serum, 10 to 5000ng/ml in milk and 25 to 1000 ng/ml in phosphate buffer. All the standard curves showed an intraday and interday variability of <10% and r^2>0.99. Twenty microliters of the sample was injected onto the LC-MS. Serum and milk concentrations of PAN were quantified according to standard curves.

Pharmacokinetic Calculations Systemic clearance was calculated using the following formula:

$$Cl_S = \frac{Infusion\ rate}{C_S} \qquad \text{Eq. 2}$$

where C_S is the average concentration of PAN in serum from 2 to 8 h. M/S was calculated by:

$$\frac{M}{S} = \frac{C_M}{C_S} \qquad \text{Eq. 3}$$

where C_M is concentration of PAN in milk at 8 h.

Statistical Analysis. Unless otherwise noted, all the data are expressed as mean ± S.D. Asymmetrical efflux ratio (ER_α) and steady state concentrations for *in vitro* flux studies as well as the protein binding and S/W data were analyzed by unpaired t-test. A p value of <0.05 was considered statistically significant. Analysis of Cls and M/S in this structured repeated measurements design (isomer, treatment, and the interaction) was performed using SAS 9.2 PROC MIXED.

Results

Pantoprazole isomers transport in rat-Abcg2 expressed in MDCKII cell line. The expression level and function of rat Abcg2-MDCKII were confirmed by Western blot, flow-cytometry and nitrofurantoin transport in previous studies (Wang et al., 2008). At 25 μM, the flux for both isomers and in both directions approached steady-state after 3 hour in empty vector and Abcg2-MDCKII cells. Initial rates were calculated during the first hour. The flux for both PAN isomers in both directions was identical in empty MDCKII cells (Figure 1A). The asymmetry efflux ratios (ER_{α}) of (+) and (-) PAN in parent cell line at the one hour time point were 0.90 and 0.95, respectively. In the Abcg2-MDCKII cell line, the initial flux rate for basolateral to apical flux was considerably greater than the flux in the opposite direction. The mass transport of (+) PAN from basolateral to apical side across monolayer appeared greater than (-) PAN (Figure 1B), whereas the flux from apical to basolateral was greater for the (-) PAN relative to the (+) PAN. The asymmetrical efflux ratio (ER_{α}) as defined (Kalvass and Pollack, 2007) for (+) and (-) PAN at the one hour time point were different ($p<0.01$) and were 5.15 and 1.51, respectively in Abcg2-MDCKII cell line. These stereoselective differences in initial rates were maintained as the profiles approached steady state of (+) and (-) PAN were 3.82 and 1.77 ($p<0.01$), respectively.

Predicted M/S ratios of pantoprazole isomers. Table 1 contains individual parameter estimates that contribute to the diffusion model prediction of M/S of the PAN isomers (Fleishaker et al., 1987). The fraction of unionized approximated 1 for both PAN isomers since their pK_a (3.9) was considerably lower than the pH of both rat milk and serum. The free fractions of PAN isomers were determined by equilibrium dialysis using serum concentrations obtained in rat infusion study. The serum free faction of (+) and (-) PAN were 2.33% and 2.38%,

DMD Fast Forward. Published on February 16, 2012 as DOI: 10.1124/dmd.111.041608
This article has not been copyedited and formatted. The final version may differ from this version.

respectively. PAN isomers have lower binding in skim milk (74% and 73%, respectively). The fat partitioning of each isomer was reflected in the S/W ratio, which was 0.75 and 0.77 for the (+) and (-) PAN, respectively. The M/S ratio predicted by the diffusion model was 0.12 for (+) PAN and 0.11 for (-) PAN.

***In vivo* study-pantoprazole isomers accumulate in rat milk.** The lactating rats were infused with racemic PAN and each isomer concentration in serum and milk were measured by LC-MS. Chromatographs of PAN isomers and zonisamide are shown in **Figure 2**.

The mean PAN isomer concentration time profiles in serum and milk are shown in **Figure 3**. In the dosing vehicle treatment, both PAN isomers appeared to achieve steady-state serum concentrations after 2 hour time point in the intravenous infusion protocol with (-) PAN (1.63 μg/ml) slightly higher than (+) PAN (1.20 μg/ml). Pre-treatment with GF120918 increased the serum concentration of both PAN isomers, in particular for (-) PAN, which increased by 37%. In the control group, (+) PAN (0.57±0.1) had greater systemic clearance (**Figure 4, panels A and B**) than did (-) PAN (0.44±0.12). The two-way ANOVA indicated a significant isomer and treatment effect, but no interaction.

At 8 hours, PAN isomers were assumed to be at steady state and were distributed differently into milk in the rat. The milk concentration of (-) PAN (2.26±0.84 μg/ml) was considerably higher than (+) PAN (0.64±0.16 μg/ml). The milk concentrations were lower for both isomers and the difference between the isomers diminished [(-) PAN (1.10±0.33 μg/ml) and (+) PAN (0.53±0.16 μg/ml)] following GF120918 administration. The M/S ratios for PAN isomers are shown in **Figure 4 (Panels C and D)**. In control (DMSO) group, M/S ratio of (-) PAN was 2.5 times that of (+) PAN. Administration of GF120918 decreased M/S ratios of (+) PAN from 0.54±0.09 to 0.38 ±0.07 and (-) PAN from 1.36±0.20 to 0.50±0.08. The two-way ANOVA

indicated a significant isomer and treatment effect, as well as a significant interaction between isomer and treatment.

DMD Fast Forward. Published on February 16, 2012 as DOI: 10.1124/dmd.111.041608
This article has not been copyedited and formatted. The final version may differ from this version.

Discussion

The current paper demonstrated that Abcg2 interacts stereoselectively with PAN isomers in both *in vitro* and *in vivo* studies which resulted in a differential accumulation of substrate isomers in milk. The M/S of (-) PAN was almost 3 times that of (+) PAN in control groups and the M/S of both isomers converged to a similar value following the administration of GF120918. Since p-glycoprotein is not expressed in lactating rat epithelium (Wang et al., 2008), this observation would indicate that Abcg2 contributes to PAN distribution in rat milk with Abcg2 serving as a major determinant for (-) PAN accumulation.

ABCG2 is a widely distributed efflux transporter and plays an important role in absorption, distribution, metabolism and excretion (ADME) of drugs and there is a growing concern regarding the role of ABCG2 in drug-drug interactions as well (Giacomini et al., 2010; Huang and Woodcock, 2010). ABCG2 has been found on the apical surface of lactating mammary epithelial cells (Jonker et al., 2005) and a number of investigators have demonstrated the importance of this transporter in the accumulation of drugs in milk (Jonker et al., 2005; Perez et al., 2009). An overarching hypothesis would hold that ABCG2 substrates accumulate in milk, resulting in relatively high M/S ratios, greater than that predicted by simple diffusion.

A clinical case report of a low M/S for PAN (Plante et al., 2004) would appear to run counter to this hypothesis since PAN is thought of a good ABCG2 substrate (Breedveld et al., 2004). The reason for the low M/S is unclear. PAN is highly protein bound (>98%) in human serum (Andersson and Weidolf, 2008) and rat serum (Xie et al., 2005). Data in the current work confirms that the protein binding of both PAN isomers in rat serum is extensive and may play some role in mitigating the contribution of rAbcg2 related accumulation in milk. PAN has a modest octanol to water partitioning and hence, the milk fat partitioning is higher (reflected in a

higher W/S value) than many drugs which should result in a higher M/S. The unionized fractions for the two isomers were assumed to be identical and were estimated to be very low and similar for skim milk and serum, hence no ion trapping influence on M/S. Therefore, the overall M/S ratios predicted by diffusion for both isomers were low and identical. The observed M/S in rat were 4.4 fold [(+) PAN] and 12.5 fold [(-) PAN] higher than predicted by diffusion, clearly suggesting a role of rAbcg2 in PAN accumulation in milk. The observed M/S ratios of (+) PAN and (-) PAN in the rat were 20-60 times higher than the M/S value reported for one lactating woman (Plante et al., 2004). The explanation for the low human M/S remains unclear.

Our *in vitro* experiment demonstrated a rAbcg2 mediated, apically directed transport of PAN and indicated that PAN is a substrate of rAbcg2, which is consistent with the reports for human and mouse ABCG2/Abcg2 (Breedveld et al., 2004; Breedveld et al., 2005). The flux of the (+) PAN was greater than the flux of the (-) PAN isomer at 25 μM (Figure 1B). Hence, one might conclude that the (+) PAN is a better substrate for rAbcg2 than (-) PAN which would contradict the *in vivo* M/S result. In order to rationalize this apparent contradiction, a more detailed *in vitro* experiment of PAN transport using a range of concentrations was performed (Wang et al., 2012). These result suggests that the (-) PAN isomer is, in fact, the better ABCG2 substrate; possessing a greater affinity and overall apical efflux permeability (PS_{AE}) for rAbcg2. The greater flux of (+) PAN (Figure 1B) arises due to the interplay between the two membranes (basolateral and apical) in determining the overall flux. At lower concentrations, PAN (both isomers) flux across the apical membrane (rAbcg2 mediated) is so rapid that the overall rate limiting step is diffusion across the basolateral membrane. At 25 μM concentration, (-) PAN isomer saturates rAbcg2 at the apical membrane, slowing its overall flux across the monolayer,

leading to the appearance of a more rapid flux for (+) PAN (Figure 1). A more comprehensive analysis is presented in companion paper (Wang et al., 2012).

In the chemical Abcg2 knockout rat model, co-administration of GF120918 decreased the systemic clearance of nitrofurantoin (Wang et al., 2008). In the present study, (-) PAN had a lower systemic clearance compared to (+) PAN and was consistent with the literature (Masubuchi et al., 1998). The administration of GF120918 had a modest effect on PAN isomer systemic clearance, which would indicate that neither Abcg2 or p-glycoprotein (also inhibited by GF1200918) play a major role in the systemic clearance of PAN. The systemic clearance of PAN in humans, is largely determined by hepatic metabolism of PAN (Huber et al., 1996).

Stereochemistry is an important aspect of biology and plays a role in many aspects of drug disposition (Bhatia et al., 2008) and yet there are few studies examining stereoselective transport of drugs (He et al., 2009; Choong et al., 2010). PAN has been used as a competitive ABCG2 inhibitor to identify other ABCG2 substrates or to study drug-drug interaction. PAN is marketed as a racemic mixture whose stereoselective disposition has been characterized (Masubuchi et al., 1998; Tanaka et al., 2001). However, the interaction of its isomers with transporters (e.g., ABCG2) has not been described. The current work clearly indicates stereoselectivity in the flux of PAN. The complexity of interpreting the *in vitro* flux data (Wang et al., 2012) might suggest that stereoselectivity may be overlooked in other transporter studies.

In conclusion, the present work has demonstrated a clear difference in the *in vivo* transport of the isomers of PAN by rAbcg2 responsible for a stereoselective difference in the accumulation of (-) PAN in milk. The current work also supports the hypothesis that ABCG2 substrates will accumulate in milk, but does not explain the previous clinical observation of a low M/S ratio. Additional studies will be needed to clarify this apparent species difference.

DMD Fast Forward. Published on February 16, 2012 as DOI: 10.1124/dmd.111.041608
This article has not been copyedited and formatted. The final version may differ from this version.

Authorship Contributions

Participated in research design: Lipeng Wang and Patrick J. McNamara

Conducted experiments: Lipeng Wang

Contributed new analytic tools: Lipeng Wang

Performed data analysis: Lipeng Wang and Patrick J. McNamara

Wrote or contributed to the writing of the manuscript: Lipeng Wang and Patrick J. McNamara

Reference

Alcorn J, Lu X, Moscow JA, and McNamara PJ (2002) Transporter gene expression in lactating and nonlactating human mammary epithelial cells using real-time reverse transcription-polymerase chain reaction. *J Pharmacol Exp Ther* **303:**487-496.

Alcorn J and McNamara PJ (2002) Acyclovir, ganciclovir, and Zidovudine transfer into rat milk. *Antimicrob Agents Chemother* **46:**1831-1836.

Andersson T and Weidolf L (2008) Stereoselective disposition of proton pump inhibitors. *Clin Drug Investig* **28:**263-279.

Bharathi DV, Hotha KK, Jagadeesh B, Chatki PK, Thriveni K, Mullangi R, and Naidu A (2009) Simultaneous estimation of four proton pump inhibitors--lansoprazole, omeprazole, pantoprazole and rabeprazole: development of a novel generic HPLC-UV method and its application to clinical pharmacokinetic study. *Biomed Chromatogr* **23:**732-739.

Bhatia P, Kolinski M, Moaddel R, Jozwiak K, and Wainer IW (2008) Determination and modelling of stereoselective interactions of ligands with drug transporters: a key dimension in the understanding of drug disposition. *Xenobiotica* **38:**656-675.

Breedveld P, Pluim D, Cipriani G, Wielinga P, van Tellingen O, Schinkel AH, and Schellens JH (2005) The effect of Bcrp1 (Abcg2) on the in vivo pharmacokinetics and brain penetration of imatinib mesylate (Gleevec): implications for the use of breast cancer resistance protein and P-glycoprotein inhibitors to enable the brain penetration of imatinib in patients. *Cancer Res* **65:**2577-2582.

Breedveld P, Zelcer N, Pluim D, Sonmezer O, Tibben MM, Beijnen JH, Schinkel AH, van Tellingen O, Borst P, and Schellens JH (2004) Mechanism of the pharmacokinetic interaction between methotrexate and benzimidazoles: potential role for breast cancer resistance protein in clinical drug-drug interactions. *Cancer Res* **64:**5804-5811.

Fleishaker JC, Desai N, and McNamara PJ (1987) Factors affecting the milk-to-plasma drug concentration ratio in lactating women: physical interactions with protein and fat. *J Pharm Sci* **76:**189-193.

Fleishaker JC and McNamara PJ (1988) In vivo evaluation in the lactating rabbit of a model for xenobiotic distribution into breast milk. *J Pharmacol Exp Ther* **244:**919-924.

Giacomini KM, Huang SM, Tweedie DJ, Benet LZ, Brouwer KL, Chu X, Dahlin A, Evers R, Fischer V, Hillgren KM, Hoffmaster KA, Ishikawa T, Keppler D, Kim RB, Lee CA, Niemi M, Polli JW, Sugiyama Y, Swaan PW, Ware JA, Wright SH, Yee SW, Zamek-Gliszczynski MJ, and Zhang L (2010) Membrane transporters in drug development. *Nat Rev Drug Discov* **9:**215-236.

Huang SM and Woodcock J (2010) Transporters in drug development: advancing on the Critical Path. *Nat Rev Drug Discov* **9:**175-176.

Huber R, Hartmann M, Bliesath H, Luhmann R, Steinijans VW, and Zech K (1996) Pharmacokinetics of pantoprazole in man. *Int J Clin Pharmacol Ther* **34:**185-194.

Jonker JW, Merino G, Musters S, van Herwaarden AE, Bolscher E, Wagenaar E, Mesman E, Dale TC, and Schinkel AH (2005) The breast cancer resistance protein BCRP (ABCG2) concentrates drugs and carcinogenic xenotoxins into milk. *Nat Med* **11:**127-129.

Kalvass JC and Pollack GM (2007) Kinetic considerations for the quantitative assessment of efflux activity and inhibition: implications for understanding and predicting the effects of efflux inhibition. *Pharm Res* **24:**265-276.

Karlsson L, Schmitt U, Josefsson M, Carlsson B, Ahlner J, Bengtsson F, Kugelberg FC, and Hiemke C (2010) Blood-brain barrier penetration of the enantiomers of venlafaxine and its metabolites in mice lacking P-glycoprotein. *Eur Neuropsychopharmacol* **20:**632-640.

Katsuki H, Hamada A, Nakamura C, Arimori K, and Nakano M (2001) Role of CYP3A4 and CYP2C19 in the stereoselective metabolism of lansoprazole by human liver microsomes. *Eur J Clin Pharmacol* **57:**709-715.

Kim J, Riggs KW, Misri S, Kent N, Oberlander TF, Grunau RE, Fitzgerald C, and Rurak DW (2006) Stereoselective disposition of fluoxetine and norfluoxetine during pregnancy and breast-feeding. *British journal of clinical pharmacology* **61:**155-163.

Mao Q and Unadkat JD (2005) Role of the breast cancer resistance protein (ABCG2) in drug transport. *Aaps J* **7:**E118-133.

Masubuchi N, Yamazaki H, and Tanaka M (1998) Stereoselective chiral inversion of pantoprazole enantiomers after separate doses to rats. *Chirality* **10:**747-753.

Merino G, Alvarez AI, Pulido MM, Molina AJ, Schinkel AH, and Prieto JG (2006) Breast cancer resistance protein (BCRP/ABCG2) transports fluoroquinolone antibiotics and affects their oral availability, pharmacokinetics and milk secretion. *Drug Metab Dispos*.

Miura M and Uno T (2009) Clinical pharmacokinetics of fexofenadine enantiomers. *Expert Opin Drug Metab Toxicol* **6:**69-74.

Oostendorp RL, Buckle T, Beijnen JH, van Tellingen O, and Schellens JH (2009) The effect of P-gp (Mdr1a/1b), BCRP (Bcrp1) and P-gp/BCRP inhibitors on the in vivo absorption, distribution, metabolism and excretion of imatinib. *Invest New Drugs* **27:**31-40.

Perez M, Blazquez AG, Real R, Mendoza G, Prieto JG, Merino G, and Alvarez AI (2009) In vitro and in vivo interaction of moxidectin with BCRP/ABCG2. *Chem Biol Interact* **180:**106-112.

Plante L, Ferron GM, Unruh M, and Mayer PR (2004) Excretion of pantoprazole in human breast. *J Reprod Med* **49:**825-827.

Tanaka M, Ohkubo T, Otani K, Suzuki A, Kaneko S, Sugawara K, Ryokawa Y, and Ishizaki T (2001) Stereoselective pharmacokinetics of pantoprazole, a proton pump inhibitor, in extensive and poor metabolizers of S-mephenytoin. *Clin Pharmacol Ther* **69:**108-113.

Tateishi T, Miura M, Suzuki T, and Uno T (2008) The different effects of itraconazole on the pharmacokinetics of fexofenadine enantiomers. *Br J Clin Pharmacol* **65:**693-700.

van Herwaarden AE, Wagenaar E, Karnekamp B, Merino G, Jonker JW, and Schinkel AH (2006) Breast cancer resistance protein (Bcrp1/Abcg2) reduces systemic exposure of the dietary carcinogens aflatoxin B1, IQ and Trp-P-1 but also mediates their secretion into breast milk. *Carcinogenesis* **27:**123-130.

Wang L, Leggas M, Empey PE, and McNamara PJ (2012) Stereoselective Interaction of Pantoprazole with ABCG2: II. In vitro flux analysis. *Drug Metab Dispos*.

Wang L, Leggas M, Goswami M, Empey PE, and McNamara PJ (2008) N-(4-[2-(1,2,3,4-tetrahydro-6,7-dimethoxy-2-isoquinolinyl)ethyl]-phenyl)-9 ,10-dihydro-5-methoxy-9-oxo-4-acridine carboxamide (GF120918) as a chemical ATP-binding cassette transporter family G member 2 (Abcg2) knockout model to study nitrofurantoin transfer into milk. *Drug Metab Dispos* **36:**2591-2596.

Xie Z, Zhang Y, Xu H, and Zhong D (2005) Pharmacokinetic differences between pantoprazole enantiomers in rats. *Pharm Res* **22:**1678-1684.

Legends

Figure 1 The amount (Mean ± SD, n=3) of PAN isomers appearing in the receiver compartment of MDCKII-empty vector and MDCKII-rAbcg2 monolayers grown on Transwells at donor concentration of 25 uM. PAN isomers: (-) PAN (open symbol) and (+) PAN (closed symbol) from the basolateral to apical (squares) and apical to basolateral (circles) in MDCKII-empty (**panel A**) and MDCKII-rAbcg2 (**panel B**). Unpaired t-test indicated a statistically significant difference of the two isomers with respect to ER_{α} and the steady state ratio ($p<0.01$).

Figure 2 Enantiomeric separation of PAN (156 ng/ml) and internal standard zonisamide (4 µg/ml) using a triple quadrupole mass spectrometer with an electrospray ionization source and a chiral column while monitoring selected product ions for PAN m/z 384 to 200 and the internal standard zonisamide m/z 213 to 132. Panels A and C represent chromatograms depicting the internal standard in PAN serum standard (156 ng/ml) and blank serum respectively. Panels B and D represent chromatograms of PAN isomers in a PAN serum standard (156 ng/ml) and blank serum (lower attenuation), respectively.

Figure 3 PAN isomer concentrations (Mean ± S.D., n=5) in serum in lactating Sprague-Dawley rats at 2, 4, 6 and 8 hour infusion (0.4 mg/ml/h infusion of racemic pantoprazole) 10 minutes following administration of dosing vehicle alone (DMSO) or GF120918 (10 mg/kg). Linear regression of serum concentration vs time showed that the slope was not significantly different from zero ($p>0.05$) indicating steady state was achieved (2-8 hr). Milk concentrations (Mean±S.D., n=5) at the end of the infusion are also shown (offset in time by 0.3 h for better visualization).

Figure 4 The averaged systemic clearance (panels A and B) and milk to serum ratio (C and D) of (+) PAN (panels A and C) and (-) PAN (panels B and D) following an infusion (0.4 mg/ml/h) of racemic pantoprazole in the presence of a bolus dose of GF120918 (10 mg/kg) or dosing vehicle alone (DMSO) administered at the initiation of the infusion. Data are presented as paired values from individual rats (n=5).

DMD Fast Forward. Published on February 16, 2012 as DOI: 10.1124/dmd.111.041608
This article has not been copyedited and formatted. The final version may differ from this version.

Table 1. Serum and milk protein binding for PAN isomers in lactating Sprague-Dawley rats (n=4). Data is presented as Mean ± S.D., unpaired t-test * $p<0.05$. Skim to whole milk partitioning ratio and diffusion model prediction of M/S (Fleishaker et al., 1987) for PAN.

Parameter	**(+) PAN**	**(-) PAN**
Fraction unbound serum (%) [a]	2.33 ± 0.51	2.40 ± 0.74
Fraction unbound milk (%) [a]	26.0 ± 2.7	27.1 ± 7.3
Whole to skim milk ratio [b]	1.33	1.3
Predicted M/S (Eq. 1)	**0.12**	**0.11**

[a] Mean ± S.D. (n=4)

[b] Single determination from a pooled sample

DMD Fast Forward. Published on February 16, 2012 as DOI: 10.1124/dmd.111.041608
This article has not been copyedited and formatted. The final version may differ from this version.

Figure 1

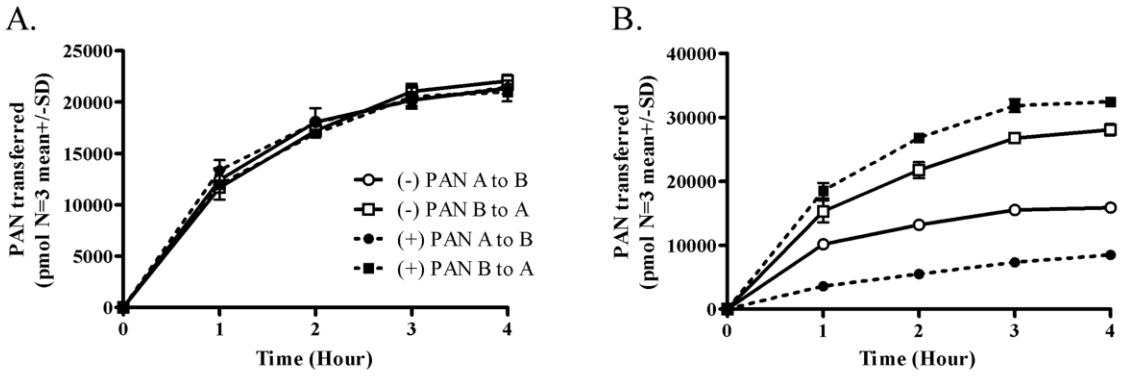

DMD Fast Forward. Published on February 16, 2012 as DOI: 10.1124/dmd.111.041608
This article has not been copyedited and formatted. The final version may differ from this version.

Figure 2

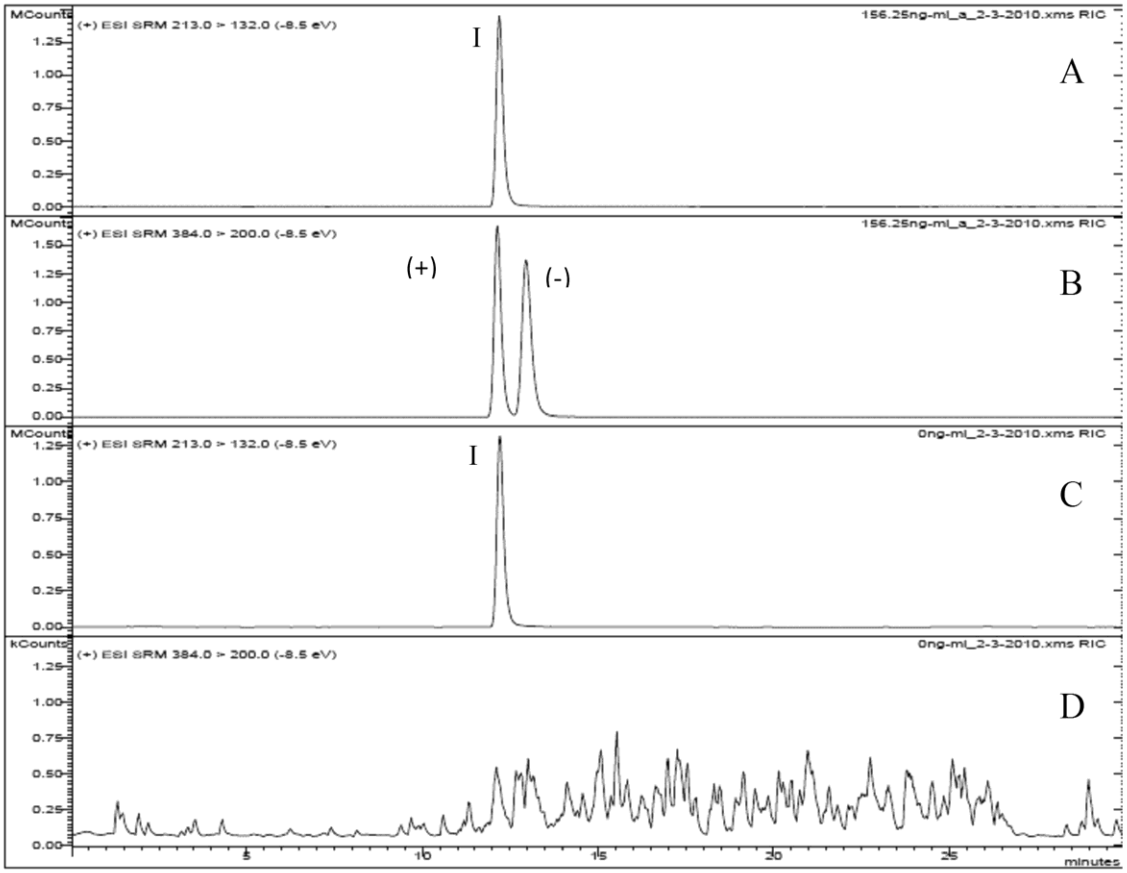

DMD Fast Forward. Published on February 16, 2012 as DOI: 10.1124/dmd.111.041608
This article has not been copyedited and formatted. The final version may differ from this version.

Figure 3

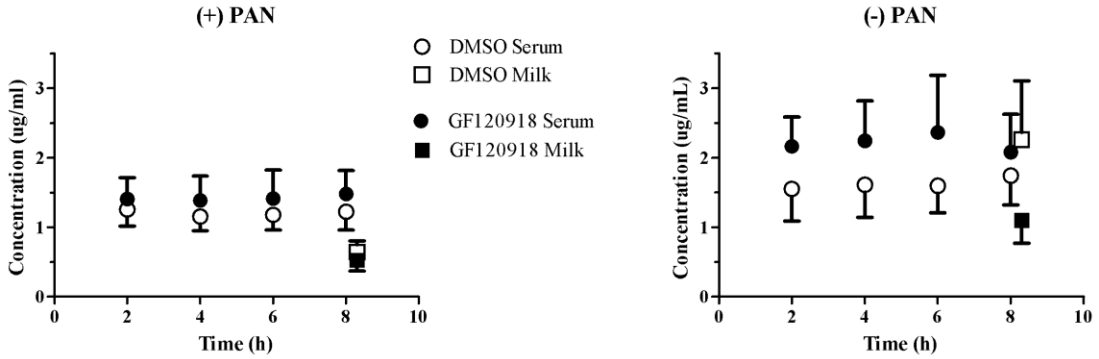

DMD Fast Forward. Published on February 16, 2012 as DOI: 10.1124/dmd.111.041608
This article has not been copyedited and formatted. The final version may differ from this version.

Figure 4